The x-ray, optical and infrared counterpart to GRB 980703

Vreeswijk, P.M.; Galama, T.J.; Owens, A.; Oosterbroek, T.; Geballe, T.R.; van Paradijs, J.; Groot, P.J.; Kouveliotou, C.; Koshut, T.; Tanvir, N.; Wijers, R.A.M.J.; Pian, E.; Palazzi, E.; Frontera, F.; Masetti, N.; Robinson, C.; Briggs, M.; in 't Zand, J.J.M.; Heise, J.; Piro, L.; Costa, E.; Feroci, M.; Antonelli, L.A.; Hurley, K.; Greiner, J.; Smith, D.A.; Levine, A.M.; Lipkin, Y.; Leibowitz, E.; Lidman, C.; Pizella, A.; Böhnhardt, H.; Doublier, V.; Chaty, S.; Smail, I.; Blain, A.; Hough, J.H.; Young, S.; Suntzeff, N.

DOI
10.1086/307740

Publication date
1999

Document Version
Final published version

Published in
Astrophysical Journal

THE ASTROPHYSICAL JOURNAL, 523:171–176, 1999 September 20

THE X-RAY, OPTICAL, AND INFRARED COUNTERPART TO GRB 980703

P. M. VREESWIJK,[1] T. J. GALAMA,[1] A. OWENS,[2] T. OOSTERBROEK,[2] T. R. GEBALLE,[3] J. VAN PARADIJS,[1,4] P. J. GROOT,[1] C. KOUVELIOTOU,[5,6] T. KOSHUT,[5,6] N. TANVIR,[7] R. A. M. J. WIJERS,[8] E. PIAN,[9] E. PALAZZI,[9] F. FRONTERA,[9,10] N. MASETTI,[9] C. ROBINSON,[4,6] M. BRIGGS,[4,6] J. J. M. in 't ZAND,[11] J. HEISE,[11] L. PIRO,[12] E. COSTA,[12] M. FEROCI,[12] L. A. ANTONELLI,[12] K. HURLEY,[13] J. GREINER,[14] D. A. SMITH,[15] A. M. LEVINE,[15] Y. LIPKIN,[16] E. LEIBOWITZ,[16] C. LIDMAN,[17] A. PIZZELLA,[17] H. BÖHNHARDT,[17] V. DOUBLIER,[17] S. CHATY,[18,19] I. SMAIL,[20] A. BLAIN,[21] J. H. HOUGH,[22] S. YOUNG,[23] AND N. SUNTZEFF[24]

Received 1998 December 14; accepted 1999 May 4

ABSTRACT

We report on X-ray, optical, and infrared follow-up observations of GRB 980703. We detect a previously unknown X-ray source in the GRB error box; assuming a power-law decline, we find for its decay index $\alpha < -0.91$ (3 σ). We invoke host-galaxy extinction to match the observed spectral slope with the slope expected from "fireball" models. We find no evidence for a spectral break in the infrared to X-ray spectral range on 1998 July 4.4, and determine a lower limit of the cooling break frequency, $\nu_c > 1.3 \times 10^{17}$ Hz. For this epoch we obtain an extinction of $A_V = 1.50 \pm 0.11$. From the X-ray data we estimate the optical extinction to be $A_V = 20.2^{+12.3}_{-7.3}$, inconsistent with the former value. Our optical spectra confirm the redshift of $z = 0.966$. We compare the afterglow of GRB 980703 with that of GRB 970508 and find that the fraction of the energy in the magnetic field, $\epsilon_B < 6 \times 10^{-5}$, is much lower in the case of GRB 980703, as a consequence of the high frequency of the cooling break.

Subject headings: gamma rays: bursts — infrared: galaxies — radiation mechanisms: nonthermal — X-rays: galaxies

1. INTRODUCTION

Several properties of gamma-ray burst (GRB) afterglows can be explained well by "fireball" models, in which a relativistically expanding shock front, caused by an energetic explosion in a central compact region, sweeps up the surrounding medium and accelerates electrons in a strong synchrotron emitting shock (Mészarós & Rees 1994; Wijers, Rees, & Mészarós 1997; Sari, Piran, & Narayan 1998; Galama et al. 1998a). The emission shows a gradual softening with time, corresponding to a decrease of the Lorentz factor of the outflow. Most X-ray and optical/infrared (IR) afterglows display a power-law decay (except GRB 980425, which is most likely associated with the peculiar supernova SN 1998bw; Galama et al. 1998b).

Spectral transitions in the optical/IR have been detected for the afterglows of GRB 970508 (Galama et al. 1998a; Wijers & Galama 1998) and GRB 971214 (Ramaprakash et al. 1998). These have been explained by the passage through the optical/IR wave band of the cooling break at ν_c (for GRB 970508) and the peak of the spectrum at ν_m (for GRB 971214); see Sari, Piran, & Narayan (1998) and Wijers & Galama (1999) for their definition. For GRB 970508, the observed break is in excellent agreement with such "fireball" models, while for GRB 971214 an exponential extinction has been invoked to explain the discrepancy between the expected and observed spectral indexes.

GRB 980703 was detected on July 3.182 UT with the All-Sky Monitor (ASM) on the *Rossi X-Ray Timing Explorer* (*RXTE*; Levine et al. 1998), the *Burst And Transient Source Experiment* (*BATSE*, trigger No. 6891; Kippen et al. 1998), *BeppoSAX* (Amati et al. 1998), and *Ulysses* (Hurley et al. 1998). The burst as seen by *BATSE* consisted of two pulses, each lasting approximately 100 s, with a total duration of about 400 s (Kippen et al. 1998). The first pulse had significant substructure, whereas the

[1] Astronomical Institute "Anton Pannekoek," University of Amsterdam; and Center for High-Energy Astrophysics, Kruislaan 403, 1098 SJ Amsterdam, The Netherlands.
[2] Astrophysics Division, Space Science Department of ESA, European Space Research and Technology Centre, 2200 AG Noordwijk, The Netherlands.
[3] Joint Astronomy Centre, 660 North A'ohoku Place, Hilo, HI 96720.
[4] Physics Department, University of Alabama in Huntsville, Huntsville AL 35899.
[5] Universities Space Research Association.
[6] NASA Marshall Space Flight Center, Code ES-84, Huntsville AL 35812.
[7] Institute of Astronomy, Madingley Road, Cambridge CB3 0HA, UK.
[8] Astronomy Program, State University of New York, Stony Brook, NY 11794-3800.
[9] Istituto Tecnologie e Studio Radiazioni Extraterrestri (TESRE), CNR, Via P. Gobetti 101, 40 129 Bologna, Italy.
[10] Dipartimento di Fisica Universita' di Ferrara, Via Paradiso 12, 44100 Ferrara, Italy.
[11] Space Research Organisation Netherlands (SRON), Sorbonnelaan 2, 3584 CA Utrecht, The Netherlands.
[12] Istituto di Astrofisica Spaziale, CNR, Via Fosso del Cavaliere, Roma, I-00133, Italy.
[13] University of California at Berkeley, Space Sciences Laboratory, Berkeley, CA 94720-7450.
[14] Astrophysikalisches Institut Potsdam, D-14482 Potsdam, Germany.
[15] Massachusetts Institute of Technology, 77 Massachusetts Avenue, Cambridge, MA 02139-4307.
[16] Wise Observatory, Tel Aviv University, Ramat Aviv, Tel Aviv 69978, Israel.
[17] European Southern Observatory, Casilla 19001, Santiago 19, Chile.
[18] DAPNIA/Service d'Astrophysique, CEA/Saclay, F-91191 Gif-Sur-Yvette, France.
[19] Centre d'Etude Spatiale des Rayonnements, 9 avenue du Colonel Roche BP 4346, F-31 028 Toulouse Cedex 4, France.
[20] University of Durham, South Road, Durham, DH1 3LE, UK.
[21] Cavendish Laboratory, Madingley Road, Cambridge CB3 0HE, UK.
[22] Physics and Astronomy, University of Hertfordshire, Hatfield, AL10 9AB, UK.
[23] Cerro Tololo Inter-American Observatory, Casilla 603, La Serena, Chile.
[24] See also http://astro.berkeley.edu/davis/dust/index.html.

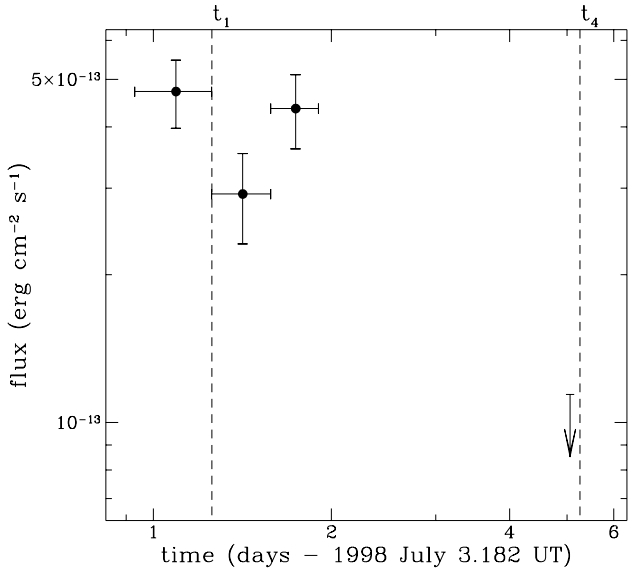

FIG. 1.—2–10 keV light curve of GRB 980703. Time and flux are on a logarithmic scale.

second, weaker episode was relatively smooth. This double-peak morphology has also been seen with the *BeppoSAX* Gamma-Ray Burst Monitor (GRBM; Amati et al. 1998). *BATSE* measured a peak flux of $(1.9 \pm 0.1) \times 10^{-6}$ ergs cm^{-2} s^{-1} (25–1000 keV) and fluence of $(4.6 \pm 0.4) \times 10^{-5}$ ergs cm^{-2} (>20 keV), consistent with the *BeppoSAX* GRBM measurement. A time-resolved spectral analysis of the burst will be presented elsewhere (Koshut et al. 1999).

Observations with the Narrow-Field Instruments (NFIs) of *BeppoSAX* showed a previously unknown X-ray source (Galama et al. 1998c) inside both the ASM error box and the interplanetary network annulus (Hurley et al. 1998). Frail et al. (1998a; see also Zapatero Osorio et al. 1998) subsequently reported the discovery of a radio (6 cm) and optical (*R*-band) counterpart to GRB 980703.

Here we report X-ray (0.1–10 keV), optical (*VRI*), and infrared (*JHK*) follow-up observations of GRB 980703. In § 2 we report our NFI X-ray observations of the ASM error box, and § 3 is devoted to the description and results of our spectroscopic and photometric optical/IR monitoring campaign. We discuss the results of these observations in § 4.

2. X-RAY OBSERVATIONS

We observed the ASM error box of GRB 980703 with the *BeppoSAX* Low- and Medium-Energy Concentrator Spectrometers (LECS, 0.1–10 keV, Parmar et al. 1997; MECS, 2–10 keV, Boella et al. 1997) on July 4.10–5.08 UT (starting 22 hr after the burst) and on July 7.78–8.71 UT. The LECS and MECS data show a previously unknown X-ray source, 1SAX J2359.1+0835, at R.A. = $23^h59^m06^s.8$, decl. = $+08°35'45''$ (equinox J2000.0), with an error radius of 50″. The field also contains the sources 1SAX J2359.9+0834 at R.A. = $23^h59^m59^s$, decl. = $+08°34'03''$, and 1SAX J0000.1+0817 at R.A. = $00^h00^m04^s$, decl. = $+08°17'14''$. Both are outside the ASM error box, do not show any variability, and coincide with the known *ROSAT* sources 1RXS J235959.1+083355 and 1RXS J000007.0+081653, respectively.

We extracted 1SAX J2359.1+0835 data at the best-fit centroids with radii of 8′ (LECS) and 2′ (MECS). To analyze the spectrum, we binned the data into channels such that each contained at least 20 counts. Using the separate standard background files of the spectrometers, we simultaneously fitted the LECS and MECS data of July 4–5 UT with a power-law spectrum and a host-galaxy absorption cutoff, using a redshift of $z = 0.966$ (Djorgovski et al. 1998; see also § 3 of this paper). In the fit we fixed the Galactic foreground absorption at $N_H = 3.4 \times 10^{20}$ cm^{-2} ($A_V = 0.19$, as inferred from the dust maps of Schlegel, Finkbeiner, & Davis 1998,[24] and the A_V-N_H relation of Predehl & Schmitt 1995). The average spectrum can be modeled with a photon index $\Gamma = 2.51 \pm 0.32$ and a host-galaxy column density $N_H(\text{host}) = 3.6^{+2.2}_{-1.3} \times 10^{22}$ cm^{-2}, corresponding to $A_V(\text{host}) = 20.2^{+12.3}_{-7.3}$ (local to the absorber). Modeling the spectrum without N_H(host) results in a very poor fit. We did not account for a possible small position-dependent error in the relative flux normalizations between the LECS and MECS, which is only a few percent near the center of the image. A change of 25% in the assumed Galactic foreground absorption does not affect the output values of the fit parameters. For the second epoch of NFI observations, we kept the position fixed at the position determined from the first epoch; we find $F_X < 1.1 \times 10^{-13}$ ergs cm^{-2} s^{-1} (3 σ). Fitting a power-law model to the light curve including the upper limit, we obtain $\alpha < -0.91$ for the decay index. The X-ray light curve is shown in Figure 1. We checked for the presence of the 6.4 keV *K* line at the redshifted energy of 3.26 keV, but did not detect it. The upper limit on its flux is 8.3×10^{-6} photons cm^{-2} s^{-1} (90% confidence level), corresponding to an equivalent width of 532 eV in the observer's frame.

3. OPTICAL AND INFRARED OBSERVATIONS

We observed the field of GRB 980703 with the Wise Observatory 1 m telescope (in *I*); the 3.5 m New Technology Telescope (NTT; in *V*, *I*, and *H*), 2.2 m (in *H* and K_s), and Dutch 90 cm (in Gunn *i*) telescopes of ESO (La Silla); the CTIO 0.9 m telescope (in *R*); and UKIRT (in *H*, *J*, and *K*).

The optical images were bias-subtracted and flat-fielded in the standard fashion. The infrared frames were reduced by first removing bad pixels and combining about five frames around each object image to obtain a sky image. This sky image was then subtracted after scaling it to the object image level, and the resulting image was flat-fielded. Four reference stars were used to obtain the differential magnitude of the optical transient (OT) in each frame. These stars were calibrated by observing the standard stars PG 2331+055 (in *V* and *I*; Landolt 1992), FS 2, and FS 32 (in *J*, *H*, and *K*; Casali & Hawarden 1992). We used the *R*-band calibration of Rhoads et al. (1998). The offsets in right ascension and declination from the OT and the apparent standard magnitudes outside the Earth's atmosphere of the reference stars are listed in Table 1.

The light curves of the OT are shown in Figure 2 (see Table 2 for a list of the magnitudes). In view of the flattening of the light curves after $t \sim 5$ days, we fitted a model $F_\nu = F_0 t^\alpha + F_{\text{gal}}$ to our own *I*- and *H*-band light curves (in these bands we have sufficient data for a free-parameter fit). Here *t* is the time since the burst in days, and F_{gal} is the flux of the underlying host galaxy. The values for $m_0 = -2.5 \log (F_0) + C$, the decay index α, and $m_{\text{gal}} = -2.5 \log (F_{\text{gal}}) + C$ are listed in Table 3. The photometric calibration, which determines *C*, has been taken from Bessell (1979) for *V*, *R*, and *I*,

TABLE 1

MAGNITUDES AND OFFSET FROM THE OT OF THE FOUR COMPARISON STARS USED

Parameter	Star 1	Star 2	Star 3	Star 4
Δ R.A. (arcsec)	−18.0	−11.7	−8.0	−13.9
Δ Decl. (arcsec).....	3.9	−9.7	−21.7	−31.8
Filter:				
V	21.33 ± 0.06	17.02 ± 0.05	22.06 ± 0.08	22.68 ± 0.12
R	20.39 ± 0.04	16.64 ± 0.02	20.72 ± 0.05	...
I	19.55 ± 0.07	16.30 ± 0.05	19.21 ± 0.06	20.01 ± 0.08
J	18.45 ± 0.13	15.75 ± 0.11	17.52 ± 0.12	18.25 ± 0.13
H	17.85 ± 0.12	15.44 ± 0.10	16.96 ± 0.11	17.69 ± 0.12
K	17.71 ± 0.13	15.41 ± 0.12	16.72 ± 0.12	17.52 ± 0.13

NOTE.—The error is the quadratic average of the measurement error (Poisson noise) and a constant offset, which we estimate to be 0.05 for the optical passbands and 0.1 for the infrared filters.

and from Bessell & Brett (1988) for *J*, *H*, and *K*. The weighted mean value of α for the *I* and *H* bands is -1.61 ± 0.12, while an *I*- and *H*-band joint fit, with a single power-law decay index, gives $\alpha = -1.63 \pm 0.12$ ($\chi = 15.4/16$). For the *V*, *R*, *J*, and *K* bands, we fixed α at -1.61, included data from the literature, and fitted m_0 and m_{gal}. The fits are shown as solid lines in Figure 2. We note that when we fit all three parameters to the *R*-band data (mainly data from the literature), we obtain a temporal slope of -1.94 ± 0.22, consistent with the adopted value of -1.61 ± 0.12. However, we do not include this value in the average, since the *R*-band magnitudes are taken from the literature and thus not consistently measured.

For four epochs we have reconstructed the spectral flux distribution of the OT (times t_1, t_2, t_3, and t_4 in Fig. 2, corresponding to 1998 July 4.4, 6.4, 7.6, and 8.4, respectively). The host-galaxy flux, obtained from the fits to the light curves, was subtracted. We corrected the OT fluxes for Galactic foreground absorption ($A_V = 0.19$). If more than one value per filter was available around the central time of the epoch, we took their weighted average. All values were brought to the same epoch by applying a correction using the slope of the fitted light curve. For the first epoch (t_1) we fitted the resulting spectral flux distribution with a power law, $F_\nu \propto \nu^\beta$, and find $\beta = -2.71 \pm 0.12$.

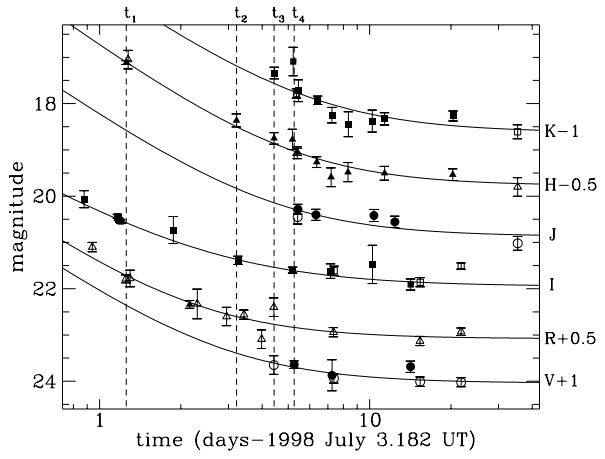

FIG. 2.—*V*, *R*, *I*, *J*, *H*, and *K* light curves of GRB 980703. The filled symbols denote our data, while the open symbols represent data taken from the literature (Zapatero Osorio et al. 1998; Rhoads et al. 1998; Henden et al. 1998; Bloom et al. 1998; Pedersen et al. 1998; Djorgovski et al. 1998; Sokolov et al. 1998; V. Sokolov et al. 1998, private communication). For each filter, a power-law model plus a constant, $F_\nu = F_0 t^\alpha + F_{gal}$, is fitted (*solid lines*). The fit parameters are listed in Table 3. The times t_1–t_4 at which we have reconstructed the spectral flux distribution of the OT are indicated by the dashed lines.

We took three 1800 s spectra of the OT with the NTT, around July 8.38 UT. The No. 3 grism that was used has a blaze wavelength of 4600 Å and a dispersion of 2.3 Å pixel^{-1}. The slit width was set at 1″. The three spectra were bias-subtracted and flat-fielded in the usual way. The coadded spectrum was then extracted the same way as the standard star Feige 110. We wavelength calibrated the spectrum with a Helium/Argon lamp spectrum, with a residual error of 0.03 Å. The spectrum was flux calibrated with the standard star Feige 110 (Massey et al. 1988). We estimate the accuracy of the flux calibration to be 10%. The wavelength- and flux-calibrated spectrum shows one clear emission line at 7330.43 ± 0.14 Å with a flux of $3.6 \pm 0.4 \times 10^{-16}$ ergs cm^{-2} s^{-1}. At the redshift $z = 0.966$ determined by Djorgovski et al. (1998) this is the λ3727 line of [O II]; our wavelength measurement corresponds to $z = 0.9665 \pm 0.0005$.

4. DISCUSSION

From the optical/IR light curves presented in § 3 we have obtained an average power-law decay constant $\alpha = -1.61 \pm 0.12$. This value is consistent with those derived by Bloom et al. (1998) ($\alpha_R = -1.22 \pm 0.35$ and $\alpha_I = -1.12 \pm 0.35$) and Castro-Tirado et al. (1999) ($\alpha_R = -1.39 \pm 0.3$ and $\alpha_H = -1.43 \pm 0.11$).

If we make the assumption that the OT emission is due to synchrotron radiation from electrons with a power-law energy distribution (with index *p*), we would expect a relation between *p*, the spectral slope β, and the decay constant α (Sari, Piran, & Narayan 1998). We assume that our observations are situated in the slow-cooling, low-frequency regime (e.g., for GRB 970508 this was already the case after 500 s; Galama et al. 1998a). One must distinguish two cases:

1. Both the peak frequency ν_m and the cooling frequency ν_c are below the optical/IR wave band. Then $p = (-4\alpha + 2)/3 = 2.81 \pm 0.16$ and $\beta = -p/2 = -1.41 \pm 0.08$.
2. The peak frequency ν_m has passed the optical/IR wave band, but ν_c has not yet. In that case, $p = (-4\alpha + 3)/3 = 3.15 \pm 0.16$ and $\beta = -(p-1)/2 = -1.07 \pm 0.08$.

In both cases, the expected value of β is inconsistent with the observed $\beta = -2.71 \pm 0.12$. Following Ramaprakash

TABLE 2

LOG OF OBSERVATIONS

UT Date (1998 July)	Magnitude	Filter	Exposure Time (s)	Seeing (arcsec)	Telescope
4.059	20.07 ± 0.19	*I*	2100	2.39	Wise 1 m
4.347	20.43 ± 0.04	*I*	900	1.16	ESO NTT (EMMI)
4.359	20.49 ± 0.03	*I*	900	1.10	ESO NTT (EMMI)
4.372	20.54 ± 0.03	*I*	900	1.14	ESO NTT (EMMI)
4.383	20.55 ± 0.04	*I*	900	1.02	ESO NTT (EMMI)
4.439	17.61 ± 0.04	*H*	810		ESO NTT (SOFI)
5.059	20.73 ± 0.29	*I*	1800	3.09	Wise 1 m
5.339	21.84 ± 0.08	*R*	3600	1.86	CTIO 0.9 m
6.395	18.86 ± 0.14	*H*	540		ESO NTT (SOFI)
7.609	19.25 ± 0.12	*H*	1200		UKIRT
7.622	18.36 ± 0.13	*K*	600		UKIRT
8.361	19.27 ± 0.22	*H*	2700		ESO 2.2 m
8.375	21.60 ± 0.06	*I*	900	0.92	ESO NTT (EMMI)
8.396	18.14 ± 0.35	K_s	2700		ESO 2.2 m
8.438	22.64 ± 0.08	*V*	900	1.93	ESO NTT (EMMI)
8.578	19.54 ± 0.08	*H*	1620		UKIRT
8.608	20.28 ± 0.10	*J*	2160		UKIRT
8.633	18.77 ± 0.24	*K*	600		UKIRT
9.509	20.40 ± 0.12	*J*	2160		UKIRT
9.554	19.76 ± 0.12	*H*	2160		UKIRT
9.614	18.94 ± 0.09	*K*	2160		UKIRT
10.353.....	21.62 ± 0.16	Gunn *i*	4800	1.22	ESO Dutch
10.380.....	20.09 ± 0.20	*H*	3750		ESO 2.2 m
10.435.....	19.24 ± 0.16	K_s	3900		ESO 2.2 m
10.440.....	22.87 ± 0.34	*V*	900	1.06	ESO NTT (EMMI)
11.496.....	19.98 ± 0.21	*H*	2160		UKIRT
11.527.....	19.47 ± 0.27	*K*	2160		UKIRT
13.414.....	18.76 ± 0.30	K_s	4950		ESO 2.2 m
13.438.....	21.47 ± 0.41	Gunn *i*	2400	1.98	ESO Dutch
13.558.....	20.42 ± 0.13	*J*	2160		UKIRT
14.536.....	20.00 ± 0.15	*H*	2160		UKIRT
14.545.....	19.36 ± 0.14	*K*	2160		UKIRT
15.582.....	20.56 ± 0.12	*J*	3240		UKIRT
17.359.....	22.68 ± 0.12	*V*	900	1.05	ESO NTT (SUSI2)
17.371.....	21.91 ± 0.12	*I*	900	0.75	ESO NTT (SUSI2)
23.501.....	20.04 ± 0.12	*H*	4860		UKIRT
23.578.....	19.28 ± 0.11	*K*	4860		UKIRT

NOTE.—Instruments and CCDs used: NTT EMMI: red arm with TEK 2k × 2k CCD (No. 36), 0.″27 pixel^{-1}; NTT SUSI2: EEV 4k × 2k CCD (No. 45 and 46), 0.″08 pixel^{-1}; NTT SOFI: Hawaii 1k × 1k HgCdTe array, 0.″29 pixel^{-1}; ESO Dutch: CCD Camera with TEK 512 × 512 CCD (No. 33), 0.″47 pixel^{-1}; Wise 1 m: TEK 1k × 1k CCD, 0.″70 pixel^{-1}; CTIO 0.9 m: TEK 2k × 2k CCD, 0.″38 pixel^{-1}; UKIRT: IRCAM3 with FPA42 256 × 256 detector, 0.″29 pixel^{-1}; 2.2 m (IRAC2b): NICMOS-3 256 × 256 array, 0.″507 pixel^{-1}. Note that we do not list an estimate of the seeing in the case of infrared observations, since the real seeing is overestimated as a result the process of coadding the individual frames.

et al. (1998), we assume that the discrepancy is caused by host-galaxy extinction (note that we have already corrected the OT fluxes for Galactic foreground absorption). To determine the host-galaxy absorption, we first blueshifted the OT flux distribution to the host-galaxy rest frame (using $z = 0.966$), and then applied an extinction correction using the Galactic extinction curve of Cardelli, Clayton, & Mathis (1989) to obtain the expected spectral slope β. For epoch t_1 (July 4.4 UT), we obtain $A_V = 1.15 \pm 0.13$ and $A_V = 1.45 \pm 0.13$ for cases 1 and 2, respectively (see Fig. 3).

TABLE 3

FIT PARAMETERS FOR THE MODEL
$m = -2.5 \log (10^{-0.4 m_0} t^{\alpha} + 10^{-0.4 m_{\rm gal}})$

Filter	m_0	α	$m_{\rm gal}$	$\chi^2_{\rm red}$
V	$21.22^{+0.48}_{-0.33}$	−1.61	$23.04^{+0.08}_{-0.08}$	5.5/5
R	$21.18^{+0.09}_{-0.08}$	−1.61	$22.58^{+0.06}_{-0.05}$	14.7/10
I	$20.60^{+0.04}_{-0.04}$	$-1.36^{+0.27}_{-0.36}$	$21.95^{+0.25}_{-0.16}$	4.5/8
J	$18.32^{+0.33}_{-0.25}$	−1.61	$20.87^{+0.07}_{-0.11}$	5.6/4
H	$17.29^{+0.06}_{-0.06}$	$-1.67^{+0.13}_{-0.15}$	$20.27^{+0.19}_{-0.15}$	6.5/7
K	$16.48^{+0.18}_{-0.15}$	−1.61	$19.62^{+0.12}_{-0.11}$	11.3/9

In case 1, we find that an extrapolation of the optical flux distribution to higher frequencies predicts an X-ray flux that is significantly below the observed value, whereas in case 2 the extrapolated and observed values are in excellent agreement. The mismatch in case 1 is in a direction that cannot be interpreted in terms of the presence of a cooling break between the optical and X-ray wave bands. When we include the X-ray data point in the fit to obtain a more accurate determination of A_V, we find $A_V = 1.50 \pm 0.11$ and $\beta = -1.013 \pm 0.016$. We conclude that the optical/IR range is not yet in the cooling regime, and so

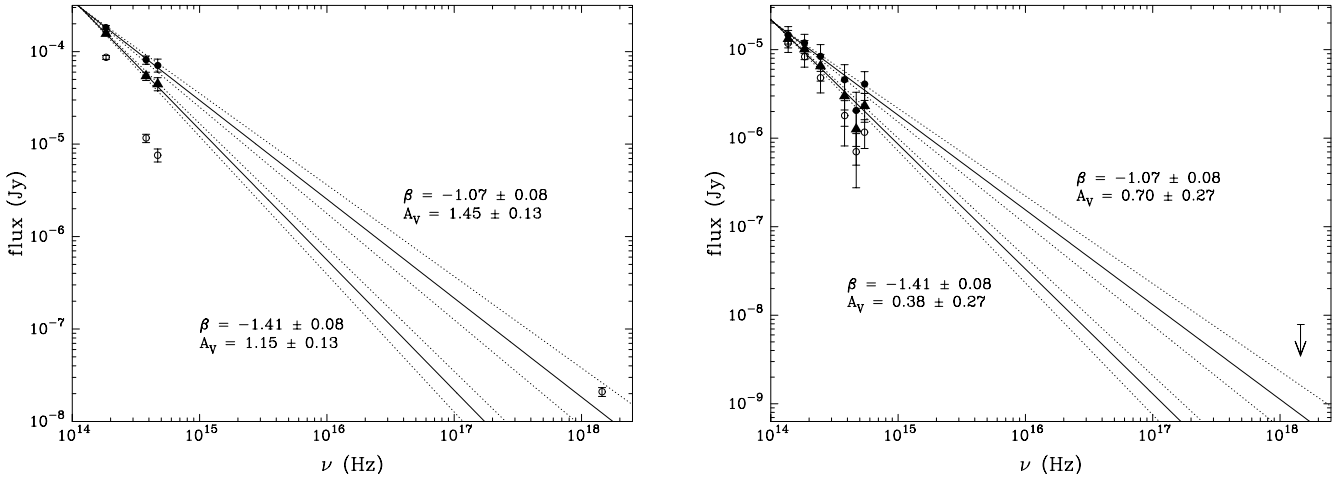

FIG. 3.—*Left*: Broadband spectrum of GRB 980703 at July 4.4 UT (i.e., at t_1 shown in Fig. 2). The open symbols show the *R*, *I*, and *H* OT fluxes (interpolated to July 4.4 and corrected for Galactic foreground absorption and the host-galaxy flux) and the MECS (2–10 keV) deabsorbed flux (the absorption correction is 7%). Filled symbols are obtained by invoking an interstellar extinction, A_V, to force the slope of the data points to take on the two possible theoretical spectral slopes. The two slopes β and their 1 σ errors are indicated by the solid and dotted lines, respectively. *Right*: Broadband spectrum of GRB 980703 at July 8.4 UT (i.e., at t_4 shown in Fig. 2). The open symbols show the *V*, *R*, *I*, *J*, *H*, and *K* OT fluxes and the MECS (2–10 keV) deabsorbed 3 σ upper limit.

$p = 3.15 \pm 0.16$. Where would the cooling frequency, ν_c, be located? The X-ray photon index, $\Gamma = 2.51 \pm 0.32$, corresponding to a spectral slope of $\beta = -1.51 \pm 0.32$, suggests that perhaps the X-ray wave band is just in the cooling regime, in which case the expected local X-ray slope would be $\beta = -p/2 = -1.57 \pm 0.08$, while if not in the cooling regime it would be $\beta = -(p-1)/2 = -1.07 \pm 0.08$. However, the large error on the measured X-ray spectral slope would also allow the cooling break to be above 2–10 keV. We estimate the (2 σ) lower limit to the cooling frequency to be $\nu_c > 1.3 \times 10^{17}$ Hz ($h\nu_c > 0.5$ keV).

We performed the same analysis for the other epoch (t_4) with X-ray data (see Fig. 3). At this epoch, the X-ray upper limit does not allow us to discriminate between the two cases. However, we can still estimate a lower limit to the cooling break from its time dependence: $\nu_c \propto t^{-1/2}$, which would allow the break to drop to $\nu_c > 6.3 \times 10^{16}$ Hz only, between epochs t_1 and t_4.

On the basis of our analysis, we conclude that there is no strong evidence for a cooling break between the optical/IR and the 2–10 keV passband before 1998 July 8.4 UT. This conclusion is at variance with Bloom et al. (1998), who infer from their fits that there is a cooling break at about 10^{17} Hz. However, upon closer inspection, there is no real disagreement; Bloom et al. found a slightly shallower temporal decay, and therefore a bluer spectrum of the afterglow, which causes their extrapolated optical spectrum to fall above the X-ray point. However, their error of 0.35 on the temporal decay leads to an error of 0.24 on their predicted spectral slope, and this means that a 1 σ steeper slope in their Fig. 2 would be consistent with no detected cooling break.

Assuming that the spectral slope ($\beta = -1.013 \pm 0.016$) did not change during the time spanned by the four epochs t_1–t_4 (as suggested by the lack of evidence for a break in the light curve during this time span), we have derived the *V*-band extinction A_V as a function of time: $A_V = 1.50 \pm 0.11$, 1.38 ± 0.35, 0.84 ± 0.29, and 0.90 ± 0.25 for the epochs 1–4, respectively. Fitting a straight line through these, we obtain a slope of -0.16 ± 0.06, i.e., not consistent with zero at the 98.8% confidence level. Such a decrease of the optical extinction, A_V, might be caused by ionization of the surrounding medium (Perna & Loeb 1997).

The *V*-band extinction $A_V = 20.2^{+12.3}_{-7.3}$, derived from the host galaxy $N_{\rm H}$ fit to the MECS and LECS data (July 4–5 UT) is not in agreement with the $A_V = 1.50 \pm 0.11$ derived from the fit from the optical spectral flux distribution. This may be due to a different dust-to-gas ratio for the host galaxy of GRB 980703 or to a higher abundance than normal of the elements that cause the X-ray absorption.

With the constraint on ν_c derived above, we can partially reconstruct the broadband flux distribution of the afterglow of GRB 980703; from the radio observations of Frail et al. (1998b) at 1.4, 4.86, and 8.46 GHz, we determine the self-absorption frequency, ν_a, and its flux, F_{ν_a}, from the fit $F_\nu = F_{\nu_a}(\nu/\nu_a)^2\{1 - \exp[-(\nu/\nu_a)^{-5/3}]\}$ to the low-energy part of the spectrum (e.g., Granot, Piran, & Sari 1998). We have

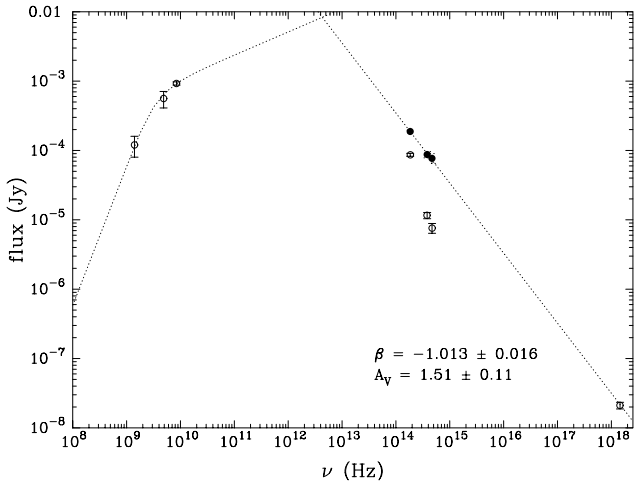

FIG. 4.—Radio to X-ray spectrum of GRB 980703 at July 4.4 UT (i.e., at t_1 shown in Fig. 2). Shown are data from Fig. 3 as well as 1.4, 4.86, and 8.46 GHz observations from Frail et al. (1998b). The fit $F_\nu = F_{\nu_a}(\nu/\nu_a)^2\{1 - \exp[-(\nu/\nu_a)^{-5/3}]\}$ to the low-energy part of the spectrum with $\nu_a = 3.68 \pm 0.33$ GHz and $F_{\nu_a} = 789 \pm 42$ μJy is shown by the dotted line. The best fit to the optical/IR and X-ray data is also shown.

used averages of the 1.4 and 4.86 GHz observations to obtain best estimates of the radio flux densities, since those frequencies in particular suffer from large fluctuations due to interstellar scintillation (Frail et al. 1998b). We find $\nu_a = 3.68 \pm 0.33$ GHz and $F_{\nu_a} = 789 \pm 42$ μJy. (The fit is shown in Fig. 4.) The intersection of the extrapolation from the low-frequency to the high-frequency fit gives a rough estimate of the peak frequency, $\nu_m \sim 4 \times 10^{12}$ Hz, and of the peak flux, $F_{\nu_m} \sim 8$ mJy (see Fig. 4). By assuming such a simple broken power law spectrum, the peak flux density will likely be overestimated (realistic spectra are rounder at the peak); it is clear from Figure 4 that $1 < F_{\nu_m} < 8$ mJy.

Following the analysis of Wijers & Galama (1999), we have determined the following intrinsic fireball properties: (1) the energy of the blast wave per unit solid angle, $\mathscr{E} > 5 \times 10^{52}$ ergs per 4π sr; (2) the ambient density, $n > 1.1$ nucleons cm^{-3}; (3) the percentage of the nucleon energy density in electrons, $\epsilon_e > 0.13$; and (4) the percentage in the magnetic field, $\epsilon_B < 6 \times 10^{-5}$. The very low energy in the magnetic field, ϵ_B, is a natural reflection of the high frequency of the cooling break, ν_c.

We have compared this afterglow spectrum with that of GRB 970508. Scaling the latter in time according to $\nu_a \propto t^0$, $\nu_m \propto t^{-3/2}$, and $\nu_c \propto t^{-1/2}$, the results of GRB 970508 (Galama et al. 1998a; see also Granot, Piran, & Sari 1998) would correspond to $\nu_a \sim 2.3$ GHz, $\nu_m = 2.8 \times 10^{12}$ Hz, $\nu_c = 4.8 \times 10^{14}$ Hz, and $F_{\nu_m} = 1.3$ mJy. In this calculation we have corrected for the effect of redshift (see Wijers & Galama 1999) such that the values represent GRB 970508, were it at the redshift of GRB 980703 and observed 1.2 days after the event. The greatest difference between the two bursts is in the location of the cooling frequency, ν_c.

The observations on the United Kingdom Infrared Telescope, which is operated by the Joint Astronomy Centre on behalf of the UK Particle Physics and Astronomy Research Council, were carried out in Service mode by UKIRT staff. The *BeppoSAX* satellite is a joint Italian and Dutch program. P. M. V. is supported by the NWO Spinoza grant. T. J. G. is supported through a grant from NFRA under contract 781.76.011. C. K. acknowledges support from NASA grant NAG5-2560. T. O. acknowledges an ESA fellowship. K. H. is grateful for support under JPL contract 958056 for *Ulysses*, and under NASA grant NAG5-1560 for IPN operations.

REFERENCES

Amati, L., et al. 1998, GCN Circ. 146 (http://gcn.gsfc.nasa.gov/gcn/gcn3/146.gcn3)
Bessell, M. S. 1979, PASP, 91, 589
Bessell, M. S., & Brett, J. M. 1988, PASP, 100, 1134
Bloom, J. S., et al. 1998, ApJ, 508, L21
Boella, G., et al. 1997, A&AS, 122, 299
Cardelli, J. A., Clayton, G. C., & Mathis, J. S. 1989, ApJ, 345, 245
Casali, M. M., & Hawarden, T. G. 1992, JCMT-UKIRT Newsl., 3, 33
Castro-Tirado, A. J., et al. 1999, ApJ, 511, L85
Djorgovski, S. G., et al. 1998, ApJ, 508, L17
Frail, D. A., et al. 1998a, GCN Circ. 128 (http://gcn.gsfc.nasa.gov/gcn/gcn3/128.gcn3)
———. 1998b, GCN Circ. 141 (http://gcn.gsfc.nasa.gov/gcn/gcn3/141.gcn3)
Galama, T. J., et al. 1998a, ApJ, 500, L97
———. 1998b, Nature, 395, 670
———. 1998c, GCN Circ. 127 (http://gcn.gsfc.nasa.gov/gcn/gcn3/127.gcn3)
Granot, J., Piran, T., & Sari, R. 1998, ApJ, submitted (astro-ph/9808007)
Henden, A. A., et al. 1998, GCN Circ. 131 (http://gcn.gsfc.nasa.gov/gcn/gcn3/131.gcn3)
Hurley, K., et al. 1998, GCN Circ. 125 (http://gcn.gsfc.nasa.gov/gcn/gcn3/125.gcn3)
Kippen, M., et al. 1998, GCN Circ. 143 (http://gcn.gsfc.nasa.gov/gcn/gcn3/143.gcn3)
Koshut, T., et al. 1999, in preparation
Landolt, A. U. 1992, AJ, 104, 340
Levine, A., et al. 1998, IAU Circ. 6966
Massey, P., et al. 1988, ApJ, 328, 315
Mészarós, P., & Rees, M. J. 1994, MNRAS, 269, L41
Parmar, A. N., et al. 1997, A&AS, 122, 309
Pedersen, H., et al. 1998, GCN Circ. 142 (http://gcn.gsfc.nasa.gov/gcn/gcn3/142.gcn3)
Perna, R., & Loeb, A. 1998, ApJ, 501, 467
Predehl, P., & Schmitt, J. H. M. M. 1995, A&A, 293, 889
Ramaprakash, A. N., et al. 1998, Nature, 393, 43
Rhoads, J., et al. 1998, GCN Circ. 144 (http://gcn.gsfc.nasa.gov/gcn/gcn3/144.gcn3)
Sari, R., Piran, T., & Narayan, R. 1998, ApJ, 497, L17
Schlegel, D. J., Finkbeiner, D. P., & Davis, M. 1998, ApJ, 500, 525
Sokolov, V., et al. 1998, GCN Circ. 147 (http://gcn.gsfc.nasa.gov/gcn/gcn3/147.gcn3)
Wijers, R. A. M. J., & Galama, T. J. 1999, ApJ, this issue
Wijers, R. A. M. J., Rees, M. J., & Mészarós, P. 1997, MNRAS, 288, L51
Zapatero Osorio, M. R., et al. 1998, IAU Circ. 6967 (http://gcn.gsfc.nasa.gov/gcn/gcn3/147.gcn3)